CHAPTER 12.

Using LiDAR to Evaluate Forest Landscape and Health Factors and Their Relationship to Habitat of the Endangered Mount Graham Red Squirrel on the Coronado National Forest, Pinaleño Mountains, Arizona[1]

(Project INT–EM–F–08–02)

John Anhold
Brent Mitchell
Craig Wilcox
Tom Mellin
Melissa Merrick
Ann Lynch
Mike Walterman
Donald Falk
John Koprowski
Denise Laes
Don Evans
Haans Fisk

[1]This work was previously published as Mitchell and others (2012) and parts of that report are included here in their entirety in this summary by the same authors.

INTRODUCTION

The Pinaleño Mountains in southeastern Arizona represent a Madrean sky island ecosystem that contains the southernmost expanse of spruce-fir forest type in North America. This ecosystem is also the last remaining habitat for the Mt. Graham red squirrel (*Tamiasciurus hudsonicus grahamensis*), a federally listed endangered species. Due to a general shift in species composition and forest structure of spruce-fir type forests across the Southwest, the ecosystem is being threatened by large high-severity fires, insect infestation, and a general loss of biodiversity. These risk factors have led the Coronado National Forest to begin a forest restoration effort using LiDAR (light detection and ranging) as a tool for identifying habitat and cataloging forest inventory variables at a landscape level. LiDAR was identified as an efficient tool for filling the data collection needs because field data collection is restricted due to rugged terrain and safety concerns.

This Pinaleño Canopy Mapping Project was divided into three phases. Phase 1 compiled the technical specifications for the LiDAR data acquisition. A request for quotes was posted, the contract was awarded, and airborne LiDAR data collected in 2008 (Laes and others 2008).

Phase 2 evaluated the acquired LiDAR data, applied image analysis techniques, and derived several forestry-based Geographic Information System (GIS) data layers. Eighty 0.05-ha forest inventory plots were established during this phase in the 2009 field season. These data were used in the subsequent phase to establish statistical relationships between the conditions on the ground and the LiDAR data for modeling (Laes and others 2009).

Phase 3 modeled forest inventory parameters at the landscape level. Regression models were constructed using forest inventory parameters measured on field plots and their associated LiDAR canopy (plot) metrics (Mitchell and others 2012).

In addition to these three initial analysis phases, the effort has led to several ongoing research projects focusing on the Mt. Graham red squirrel and its habitat, an intended outcome of the original project proposal. Led by the University of Arizona Conservation Research Laboratory and Mount Graham Research Program, researchers have utilized the LiDAR GIS layers and modeling products from the Forest Service, U.S. Department of Agriculture Remote Sensing Applications Center (RSAC) to create additional LiDAR analysis layers and habitat models (Merrick and others 2013).

METHODS

The project area covers approximately 85,500 acres (34 600 ha) in the mixed-conifer and spruce-fir zones above 7,000 feet (2133 m) within the Pinaleño Mountains, located southwest of Safford, Graham County, Arizona (fig. 12.1).

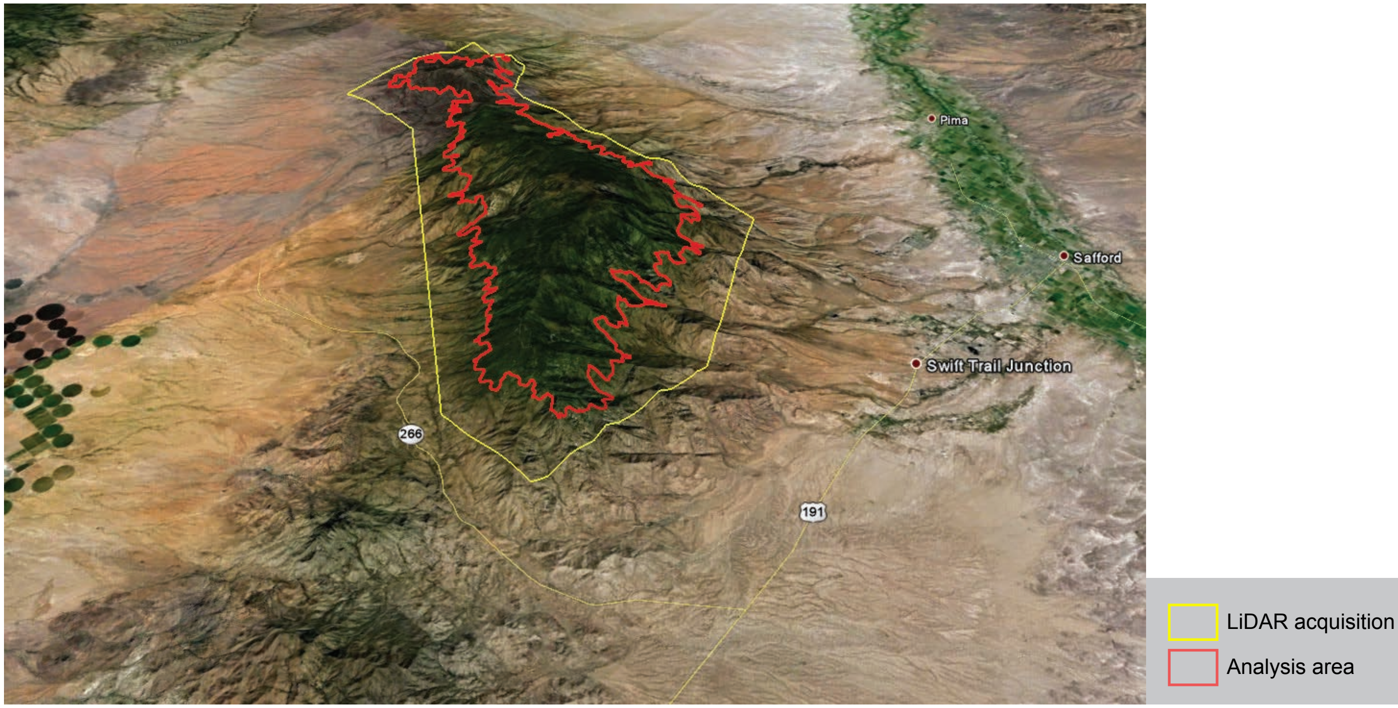

Figure 12.1—Pinaleño Mountains in southeastern Arizona showing the LiDAR acquisition and forest inventory modeling area represented in a three-dimensional virtual globe environment (Mitchell and others 2012).

Data collected for this project included airborne LiDAR data and associated field plot data. The two datasets were collected with similar dates, and field data were collected specifically for use with high-resolution LiDAR data.

LiDAR Data

High pulse-density LiDAR data were acquired over the Pinaleño Mountains project area September 22–27, 2008. The dataset had a nominal pulse density of ≥3 pulses/m^2, >50 percent side lap, and a scan angle within 14 degrees off nadir. The full LiDAR data collection specifications and quality assessment can be found in the Phase 2 report by Laes and others (2009).

Field Data

Field data were collected with the primary goal of addressing data needs to support LiDAR modeling. Eighty field plots were collected in the summer of 2009 based on a 500-m grid.

Plots were 1/20-ha (0.05-ha) fixed plots with a 12.62-m radius. Only 80 of the 200 potential plot locations were sampled due to extreme terrain, one of the primary reasons for the LiDAR project. All plots were permanently monumented and trees tagged.

Plot location maps for the 80 plots were created to assist the field crew. A color infrared aerial photo was used as a backdrop with the plots marked by a circle (fig. 12.2). LiDAR subsets were also clipped from the data, which provided the field crew an additional 3-D visualization of the desired plot location. Using map products and predetermined plot coordinates, the field crew navigated to the potential plot location using GPS. The actual plot center location and elevation were recorded using a GPS unit (Trimble® GeoXH™) capable of submeter locational accuracy. Differential corrections were used to increase plot location accuracy. A relatively high level of positional accuracy is needed

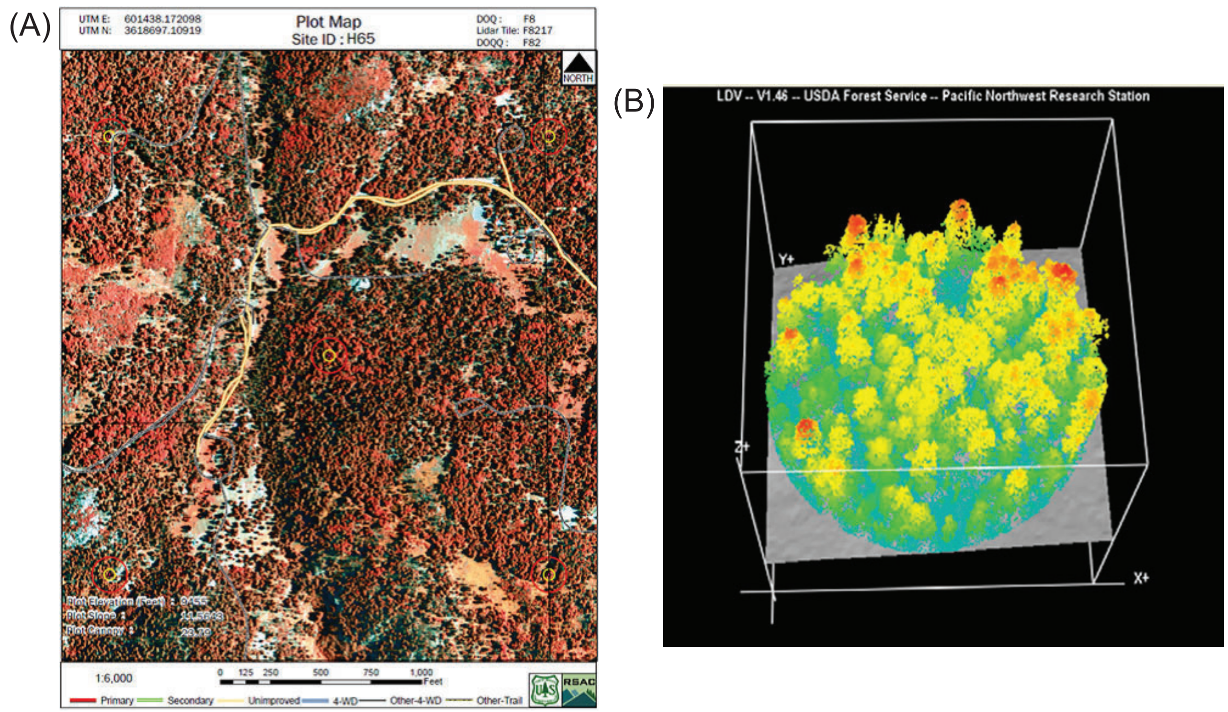

Figure 12.2—(A) Example of a map book page created for each of 80 field plots surveyed in support of the LiDAR modeling analysis for the Pinaleño Mountain study area. These map book pages helped field crews find the correct plot locations (Mitchell and others 2012). (B) Three-dimensional LiDAR point cloud visualization of the plot, which was also provided to the field crew for each potential plot location.

to minimize error and maximize correlation between field and LiDAR data in the modeling methodology.

All trees (live or dead) ≥20 cm in diameter at breast height (d.b.h.) and all coarse woody debris (down logs) >20 cm were measured on each plot. To assess smaller trees and small coarse woody fuel, a 1/60-ha wedge-shaped subplot was created within the plot from a random radius bearing. All trees (live or dead) <20 cm in d.b.h. and coarse woody debris <20 cm but ≥5 cm in diameter were measured in the subplot. Three Brown's fuel transects (Brown 1974) and understory cover transects were used to measure shrub, forbs, grasses, and regeneration. Three photos were collected at each plot location.

The LiDAR and field inventory data were then processed and prepared for modeling. The goal of the data processing was to ensure a high level of correspondence between the data sets. Field inventory data were summarized to the plot level [e.g., basal area (BA), stand density index (SDI), average tree height, trees/ha (TPH), and quadratic mean diameter (QMD)] with corresponding metrics from the LiDAR data.

LiDAR predictor variables were generated at the plot scale using FUSION software (McGaughey 2012). The ClipData FUSION command was used to subset the LiDAR data. LiDAR metrics were calculated for each plot's point cloud using FUSION's CloudMetrics command. The resulting metrics became the predictor variables for the inventory models.

In summary, the plot level data were used to develop models to estimate the forest inventory variables while LiDAR metrics at the landscape scale were used in subsequent steps to apply the regression models to the entire landscape.

Model Development

Predictive models were created for 23 different forest and fuel inventory parameters (Mitchell and others 2012). Since all parameters being modeled are represented by continuous values, regression techniques were used to perform the modeling. Nonlinear regression was used to provide adequate predictive functions for each of the modeled parameters. All models created and applied to the landscape, along with the selected LiDAR predictor variables, are displayed in table 12.1.

The modeling process was conducted in five principal stages: (1) identify best predictors, (2) create appropriate modeling masks, (3) generate forest inventory models, (4) extrapolation, and (5) validation. To find the best linear predictors, a "leave one out" cross validation with a generalized linear regression model was used to find the LiDAR-derived parameters that best predicted the plot parameters. Forty LiDAR predictor variables were evaluated for each model. Two selected as additional variables did not contribute to model performance. Once these were selected, a curve-fitting application was used to identify the best nonlinear functions to correlate the LiDAR predictors with the modeled parameters of interest. The final models that were regarded as acceptable to apply to the

Table 12.1—Summarizations of the best linear and nonlinear forest inventory models created using LiDAR predictor variables to model field-derived forest inventory parameters (Mitchell and others 2012)

Predicted	Parameter 1	Parameter 2	Linear fit-R^2	Nonlinear fit-R^2	Nonlinear equation
TotBMKg (biomass in kg/ha)	Elev mean	(all returns above mean) / (total first returns) * 100	0.7416	0.8780	z = (ax/b - cy/d) / (1 + x/b + y/d) + Offset
BAwHGT (Lorey's mean height)	Elev mean	Elev skewness	0.8123	0.8265	z = a + bx + cy + dx^2 + fy^2 + gx^3 + hy^3
CUMVolTot (volume)	Elev P60	(all returns above mean) / (total first returns) * 100	0.7026	0.8216	z = (a + b*ln(x) + c*ln(y) + d*ln(x)*ln(y))/(1 + f*ln(x) + g*ln(y) + h*ln(x)*ln(y))
BATotal (total basal area)	Elev P75	(all returns above mean) / (total first returns) * 100	0.7024	0.7782	z = a + bx + cy + dx^2 + fy^2 + gx^3 + hy^3 + ixy + jx^2y + kxy^2
SDItotal (stand density index)	Percentage all returns above 3.00	(all returns above mode) / (total first returns) * 100	0.6994	0.7614	z = a + b*y + c*y^2 + d*y^3 + f*y^4 + g*x + h*x*y + i*x*y^2 + j*x*y^3 + k*x*y^4
HGTmax (height of tallest tree)	Elev L2	Percentage all returns above 3.00	0.6919	0.7529	z = a + by + cy^2 + dy^3 + fx + gxy + hxy^2 + ixy^3
CUMVolD (volume dead)	Percentage all returns above mean	(all returns above mean) / (total first returns) * 100	0.4038	0.7361	z = (a + b*ln(x) + c*exp(y) + d*ln(x)exp(y))/(1 + fx + gy + hxy) + Offset
SdHGT (std tree height)	Elev variance	Elev P50	0.5802	0.6817	z = (a + bx + cy + dxy)/(1 + f*ln(x) + g*ln(y) + h*ln(x)*ln(y)) + Offset
BALive (live basal area)	Percentage all returns above mean	—	0.5993	0.67	z = 0.0153*x^2 + 0.9306*x - 3.8899
CBH (canopy base height)	Elev variance	Elev CV	0.4855	0.6187	z = (a + b*exp(x) + c*exp(y) + d*v(x)exp(y))/(1 + fx + gy + hxy) + Offset
CFL (canopy fuel load)	Percentage all returns above mean	(all returns above mode) / (total first returns) * 100	0.512	0.6	z = (a + bx + cy + dxy)/(1 + f*ln(x) + g*ln(y) + h*ln(x)*ln(y)) + Offset
QMD[a] (quadratic mean diameter)	Elev minimum	Elev P10	0.3932	0.4909	z = (a + bx + cy + dxy)/(1 + f*ln(x) + g*ln(y) + h*ln(x)*ln(y))
*CBD[a] (canopy bulk density)	Elev P20	Percentage all returns above mean	0.3724	0.4378	z = (a + bx + cy + dxy)/(1 + f*ln(x) + g*ln(y) + h*ln(x)*ln(y)) + Offset

— = no parameter 2 exists for BALive.

[a] Model did not meet the R^2 threshold of 0.6, but was included based on interest of cooperators.

landscape based on a smoothness of fit and an R^2 value ≥0.6 are displayed in table 12.1. The models for quadratic mean diameter and canopy bulk density were included for further investigation based on interest from the project cooperators even though the models did not meet the R^2 threshold.

Some of the forest inventory parameters that performed poorly included downed woody fuels, TPH, and QMD. The poor performance of downed woody fuels models probably reflects the limitation of LiDAR ground-filtering models to differentiate between the modeled ground surface and coarse woody debris. TPH and QMD are difficult to estimate due to the large variation in tree size. Both QMD and TPH could have benefited from a second round of modeling in which trees under a certain diameter class (<5 cm) were excluded from the model. This is typically done in traditional forest inventories where numerous small trees wash out the midstory and overstory characteristics of the unit being measured. Parameters governed by larger tree size, such as BA, SDI, volume, biomass, and Lorey's mean height, performed well in our study. Lorey's mean tree height (height of a tree of average BA) holds particular promise (R^2 = 0.83) with LiDAR inventories and could be used in a similar fashion as QMD to represent the average tree of a stand. Since all tree heights within the plots were measured, we were able to calculate Lorey's mean tree height and develop models for this parameter.

LiDAR may be superior to field estimates at measuring parameters that are indirectly measured in the field, such as crown bulk density, but ascertaining this will require more intensive studies. For example, crown bulk density is estimated from very costly whole tree clipping studies but can be mathematically modeled using more easily measured tree attributes (height, diameter, and species). Clipping studies utilizing LiDAR data may be required to develop better models.

Our models for estimating continuous forest inventory measurements across the LiDAR acquisition area performed poorly in two areas: areas that fell outside the range of plot measurements and thus required the model to extrapolate estimates, and nonforest areas. Predicted data outliers were masked and clipped in the first circumstance, and in the latter, nonforested areas were excluded from the modeling process.

Continuous inventory parameters were created at the landscape scale by applying the derived equations (table 12.1) to the LiDAR GridMetrics layers. Each calculation produced a new grid of cells with 25-m side lengths, each of which spatially represented the estimated forest parameter of interest derived from the LiDAR data (fig. 12.3). These models were validated using local biological, silvicultural, and ecological knowledge of the study area alongside ancillary GIS data and imagery.

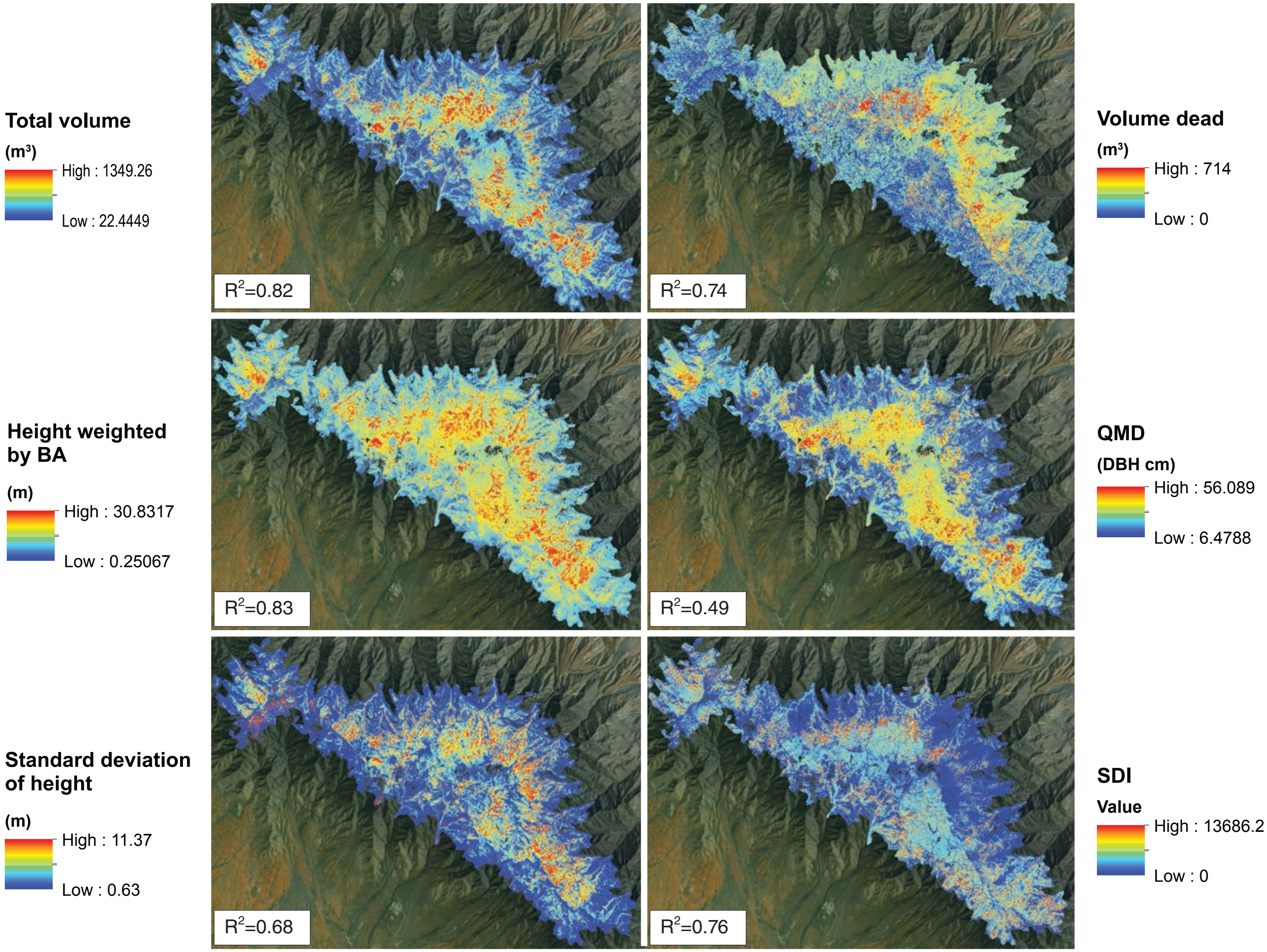

Figure 12.3—The Geographic Information System (GIS) grid layers (25-m cell size) represent the forest inventory parameter models applied at the landscape level (Mitchell and others 2012). These GIS layers are the end user products that will be used for future decisionmaking, analysis, and monitoring for the Pinaleño Mountain study area. Note: QMD = quadratic mean diameter, DBH = diameter at breast height, SDI = stand density index, BA = basal area.

Since LiDAR technology directly and continuously measures the structural characteristics of the forest vegetation across the landscape, and the modeling methodology used has been replicated and accepted internationally (Means and others 2000, Naesset 2002), we are confident that our statistically validated models provide reasonable results representing trends known to exist on the landscape.

CONCLUSIONS

The Pinaleño Canopy Mapping Project illustrates that forest inventory parameters measured in the field can be successfully modeled across the landscape with continuous LiDAR data. Parameters such as biomass (above ground), basal area, Lorey's mean height, and timber volume appear to lend themselves to this methodology, which is not surprising as they are directly related to tree size and density of vegetation. Our methodology failed to adequately model trees/ha or any of the down woody debris parameters.

The landscape GIS layers are also being used by the Coronado National Forest to create better strategies for managing and conserving the Pinaleño sky island ecosystem. The first-order LiDAR derivatives, modeled parameters, and the landscape GIS inventory layers created from this project are currently being incorporated into habitat characterization studies for the Mt. Graham red squirrel. In particular, the University of Arizona Conservation Research Laboratory's work has utilized the project's products. The lab's interests have focused on factors influencing natal dispersal movements and habitat selection during adult red squirrel settlement. The researchers are currently testing several hypotheses related to natal habitat preference within mixed conifer forest, decision rules habitat selection, habitat fragmentation, wildfire impacts, and Forest Service restoration treatments and their influence on red squirrel dispersal movements and settlement patterns. These studies utilize the Pinaleño LiDAR data in conjunction with other field-based measurements to model red squirrel occurrence and settlement, to characterize forest structure, to develop canopy connectivity indices and identify dispersal thresholds, and to identify forest structural features associated with long-term Mt. Graham red squirrel occupancy (Merrick 2014) (fig. 12.4).

This project, from scoping and data acquisition to production of usable GIS layers, took approximately 65 weeks. We have demonstrated that first-order LiDAR derivatives, such as canopy height and percent canopy cover, can be used in natural resource management activities without the added cost of field data collection and in-depth modeling scenarios described in this report. The LiDAR approach to obtaining forest structure data had several benefits over a ground-based approach. First, it provided continuous coverage of all forested areas, rather than stand- or plot-level estimates of various parameters created from stratified sampling methods. Second, it sampled areas that field crews could not safely measure due to extreme terrain. Third, it was very cost effective. The Coronado National Forest estimates that obtaining (statistically less valid and complete) data sufficient to implement the Pinaleño forest restoration project and other anticipated projects would cost approximately $500,000 (assuming that crews could safely work in all areas, which is not the case). By comparison, the Pinaleño LiDAR mapping project cost $250,000 including acquisition, processing, and analysis.

CONTACT INFORMATION

John Anhold: janhold@fs.fed.us.

LITERATURE CITED

Brown, J.K. 1974. Handbook for inventorying downed woody material. Gen. Tech. Rep. INT–16. Ogden, UT: U.S. Department of Agriculture Forest Service, Intermountain Forest and Range Experiment Station. 24 p.

Laes, D.; Reutebuch, S.; McGaughey, B. [and others]. 2008. Practical LiDAR-acquisition considerations for forestry applications. RSAC–0111–BRIEF1. Salt Lake City, UT: U.S. Department of Agriculture Forest Service, Remote Sensing Applications Center. 32 p.

Laes, D.; Mellin, T.; Wilcox, C. [and others]. 2009. Mapping vegetation structure in the Pinaleño Mountains using LiDAR. RSAC–0118–RPT1. Salt Lake City, UT: U.S. Department of Agriculture Forest Service, Remote Sensing Applications Center. 84 p.

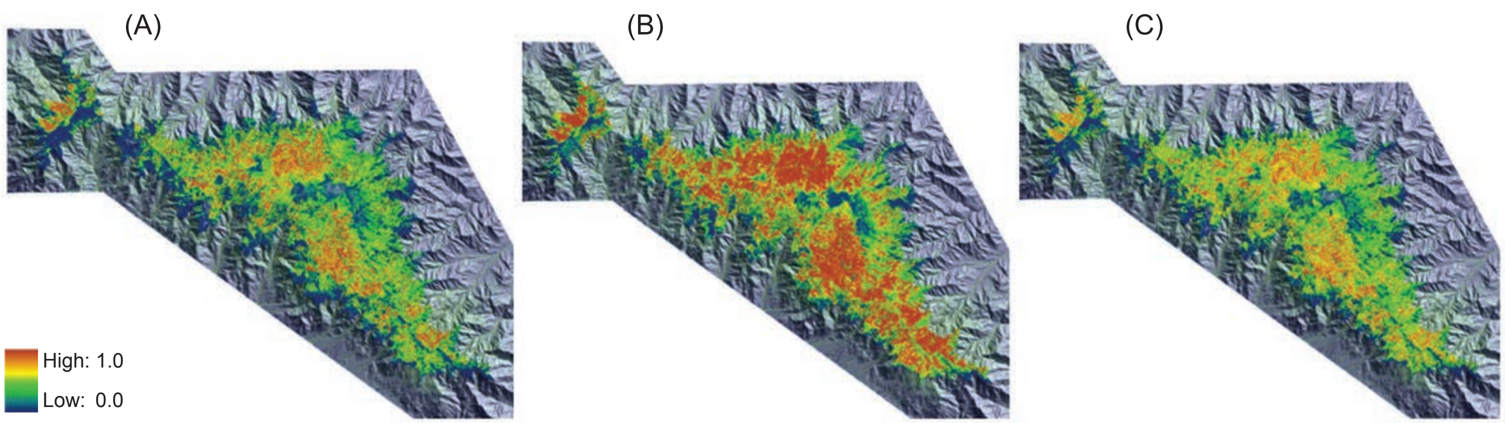

Figure 12.4—Mt. Graham red squirrel habitat maps with probability of use for (A) juveniles, (B) adults, and (C) all ages. (Source: Mitchell and others 2012)

Merrick, M.J. 2014. A new dimension for spatial ecology: LiDAR as a tool for improving wildlife habitat models and fostering collaboration. Remotely Wild: Newsletter of the Spatial Ecology and Telemetry Working Group. The Wildlife Society. Issue 30, Spring: 10-17.

Merrick, M.J.; Koprowski, J.L.; Wilcox, C. 2013. Into the third dimension: benefits of incorporating LiDAR into wildlife habitat models. In: Gottfried, G.J.; Gebow, B.S.; Eskew, L.G., eds. Biodiversity and management of the Madrean Archipelago, conference 3. Proceedings RMRS–P–67. Fort Collins, CO: U.S. Department of Agriculture Forest Service, Rocky Mountain Research Station: 389-395.

Mitchell, B.; Walterman, M.; Mellin, T. [and others]. 2012. Mapping vegetation structure in the Pinaleño Mountains using LiDAR—phase 3: forest inventory modeling. RSAC–10007–RPT1. Salt Lake City, UT: U.S. Department of Agriculture Forest Service, Remote Sensing Applications Center. 17 p.

McGaughey, R. 2012. FUSION/LDV: software for LiDAR data analysis and visualization. Version 3.01. Seattle, WA: U.S. Department of Agriculture Forest Service, Pacific Northwest Research Station. http://forsys.cfr.washington.edu/fusion/fusionlatest.html. [Date accessed: April 2, 2012].

Means, J.E.; Acker, S.A.; Fitt, B.J. [and others]. 2000. Predicting forest stand characteristics with airborne scanning LiDAR. Photogrammetric Engineering and Remote Sensing. 66(11): 1367-1371.

Naesset, E. 2002. Predicting forest stand characteristics with airborne scanning laser using a practical two-stage procedure and field data. Remote Sensing of Environment. 80: 88-99.